SERBIAN JOURNAL OF ELECTRICAL ENGINEERING
Vol. 22, No. 3, October 2025, 453-478

UDC: 004.421.6: 510.644.4 **DOI: https://doi.org/10.2298/SJEE240917008P**

Original scientific paper

Development and Application of Advanced Control Strategies for Nonlinear Coupled MIMO Systems

Alpesh Patel[1], Dipak Adhyaru[1], Jignesh Patel[1]

Abstract: This paper presents the design and implementation of advanced control algorithms for a nonlinear coupled Multi-Input Multi-Output (MIMO) system, focusing on the hardware structure of Quadruple Conical Tank System (QCTS). Nonlinear MIMO systems, characterized by complex interactions between multiple inputs and outputs, pose significant challenges for control engineering. The QCTS, with its four interconnected conical tanks, serves as an exemplary testbed for evaluating advanced control strategies. The paper elaborates on the theoretical and practical implementation of Proportional-Integral-Derivative (PID) control, Fuzzy Logic Control (FLC), and Model Predictive Control (MPC), emphasizing their capabilities in managing multi-variable systems with constraints. Additionally, a comparative analysis of MPC with traditional control methods such as PID and FLC is presented. The practical implementation is demonstrated through hardware experiments. The hardware experimental results highlight the strengths and limitations of each control strategy, providing insights into their applicability for complex nonlinear MIMO systems. The findings underscore the superior performance of MPC in handling multi-variable interactions and constraints, making it a robust choice for advanced control applications in industrial processes.

Keywords: Model predictive control, Quadruple Conical Tank System, Nonlinear system dynamics, Fuzzy logic control, PID control.

1 Introduction

Industrial processes are often intricate and it defy simple control methods. Nonlinear process control provides a sophisticated toolkit for managing complex systems. Unlike linear systems, where a change in input results in a proportional

[1]Electronics and Instrumentation Dept., Institute of Technology, Nirma University, Ahmedabad, Gujarat, India
alpesh.patel@nirmauni.ac.in, https://orcid.org/0000-0002-6206-4080
dipak.adhyaru@nirmauni.ac.in, https://orcid.org/0000-0002-7906-1978
jigneshpatel180673@gmail.com, https://orcid.org/0000-0001-9765-8375

Colour versions of the one or more of the figures in this paper are available online at https://sjee.ftn.kg.ac.rs change in output, nonlinear systems exhibit a more intricate relationship where inputs can lead to varied and sometimes unexpected output.

Imagine a chemical reactor where the reaction rate doesn't increase proportionally with temperature but jumps or even delays. Traditional control methods struggle with nonlinearities. Small adjustments can lead to unpredictable outcomes, potentially causing poor product quality, compromised safety, and wasted energy. Nonlinear process control is essential for ensuring product quality, operational safety, and energy efficiency in various industries [1]. Model Predictive Control (MPC) is a sophisticated control strategy widely employed in industrial applications to optimize system performance by predicting future behavior based on a process model and adjusting control inputs accordingly. This approach is particularly effective in scenarios where precise control is required over multiple variables simultaneously. The QCTS, known for its nonlinear dynamics, poses challenges that traditional control methods struggle to address comprehensively. MPC stands out by leveraging a detailed model that incorporates these nonlinearities, allowing it to compute optimal control actions, such as adjusting pump flow rates, to achieve desired water levels across all tanks [2]. The application of MPC in systems like the QCTS offers several advantages. Firstly, it excels in handling complex nonlinear relationships between variables and can accommodate various operational constraints effectively. This capability is crucial for maintaining stability and achieving desired performance metrics like minimizing overshoot and settling time. MPC's versatility extends to both Single-Input Single-Output (SISO) and Multiple-input Multiple-Output (MIMO) systems, making it suitable for controlling interconnected processes where interactions between variables are significant [3].

However, MPC also comes with its challenges. One major requirement is the need for an accurate model of the system dynamics. The effectiveness of MPC heavily relies on the precision of this model; inaccuracies can lead to suboptimal control performance or even instability. Moreover, MPC can be computationally intensive, especially for large-scale or complex systems.

Internal Model Control (IMC) is a control strategy that integrates an inverse model of the process within the control loop to enhance disturbance rejection and ensure robust performance. This method is particularly valued in industrial applications where maintaining stable operation despite external disturbances is crucial. In IMC, the inverse model is designed to predict the effect of disturbances on the system's output and generates control actions to counteract these disturbances effectively. For instance, in the context of the QCTS, IMC would utilize the inverse model to accurately estimate how changes in external factors, such as variations in inflow rates or tank levels, affect the system's response. By anticipating these disturbances, IMC adjusts control inputs proactively, thereby minimizing deviations from desired operating conditions and ensuring consistent performance [1].

However, IMC also presents challenges that need careful consideration. Like many model-based control approaches, IMC relies heavily on the accuracy of the process model. Any discrepancies between the actual system dynamics and the model can lead to suboptimal performance or instability. Additionally, IMC may not be as effective for highly nonlinear systems where the relationship between inputs and outputs is complex and difficult to model accurately. Despite these limitations, IMC remains a valuable tool in the control engineer's toolkit, particularly for processes where disturbance rejection and robust performance are paramount.

Robust Control, particularly through H∞ theory, represents an advanced approach in designing controllers that prioritize stability and performance resilience amidst uncertainties and disturbances within a system. The fundamental goal is to develop controllers capable of maintaining system stability and achieving desired performance metrics, even when faced with unpredictable factors such as varying pump characteristics or inaccuracies in sensor data. For instance, in the case of the QCTS, H∞ control ensures that the controller adapts to changes in operating conditions without compromising stability. By focusing on robustness, H∞ control minimizes the impact of uncertainties, ensuring reliable operation across a range of dynamic conditions.

One of the key advantages of H∞ control lies in its ability to provide consistent performance under uncertain and dynamic environments. This robustness makes it particularly suitable for systems where disturbances are prevalent or where the exact system parameters are not perfectly known. H∞ controllers are adept at mitigating the effects of disturbances by optimizing control actions to maintain system stability and achieve desired performance criteria [4]. However, the design and analysis of H∞ controllers can be complex, often requiring sophisticated mathematical models and computation-intensive algorithms. The focus on robustness can sometimes lead to conservative control strategies, where controllers prioritize stability margins over maximizing performance metrics. Balancing robustness with performance objectives is a critical consideration in applying H∞ control effectively, ensuring that the controller's design aligns with the specific operational needs and constraints of the system.

Fuzzy Logic Control (FLC) is a strategy that harnesses human-like reasoning to manage complex nonlinear systems, such as the QCTS, by using a set of linguistic rules. Unlike traditional control methods that rely heavily on precise mathematical models, FLC excels in environments where the system dynamics are intricate or difficult to model explicitly. In the context of the QCTS, the application of SISO FLC involves translating sensor data, like water level measurements from each tank, into actionable control decisions for the pumps. By encoding expert knowledge into fuzzy rules, the controller can adaptively adjust pump flow rates based on the current system state, effectively regulating water levels across all tanks [5].

One notable advantage of FLC is its ability to handle complex nonlinearities inherent in real-world systems without the need for an exact mathematical model. This flexibility makes it particularly suitable for applications where the system dynamics may change over time or are not fully understood. Additionally, while FLC excels in managing nonlinear systems, its control actions may not always be as systematic or optimal as those generated by model-based control approaches that rely on precise system models and rigorous optimization algorithms. Thus, the choice between FLC and other control strategies often hinges on the specific requirements and complexities of the application at hand.

Decentralized Control is a strategic approach that breaks down the complexity of controlling a multi-variable system, such as the QCTS, into simpler, more manageable subsystems or loops. In systems like the QCTS, where multiple tanks need to maintain specific water levels independently, decentralized control assigns a separate Proportional-Integral-Derivative (PID) controller to regulate each tank's level. This method allows for individualized control actions without requiring coordination across all system variables simultaneously. For instance, in the context of the QCTS, each tank can adjust its pump flow rate based on its own water level measurements, ensuring that deviations from setpoints are corrected autonomously [6].

One significant advantage of decentralized control is its relative simplicity in design and implementation, especially for systems with multiple interacting variables. By breaking down the control problem into smaller sub-problems, engineers can focus on optimizing each PID controller for its specific task without the computational burden of managing a centralized control scheme. Moreover, decentralized control strategies can offer robustness against failures in one part of the system. If one PID controller malfunctions or encounters disturbances, the others can continue operating independently, potentially mitigating the impact on overall system performance [7]. However, decentralized control may not always achieve the same level of performance optimization as centralized approaches. It can be challenging to manage interactions between variables across different control loops, which may lead to suboptimal coordination and responsiveness in dynamically changing environments [11]. The controlled variable is the liquid level in the bottom two tanks.

2 Mathematical Modeling

The mathematical modelling of control systems is a critical step in understanding and analyzing the dynamic behavior of a process [14]. The quadruple conical tank system is a four interconnected tank process with two pumps as shown in Fig. 1. The QCTS setup consists of four conically shaped interconnected tanks. The focus of control in this study is on the bottom two tanks (Tank 1 and Tank 2), while the top two tanks serve as intermediate storage feeding into the lower ones. The two final control element voltages (0 – 5 V) serve as the process inputs, while the levels of the bottom two tanks–measured as sensor voltages (0 – 5 V) –represent the outputs. The motive is to control the levels of the bottom two tanks by controlling the input of final control element's voltage [8].

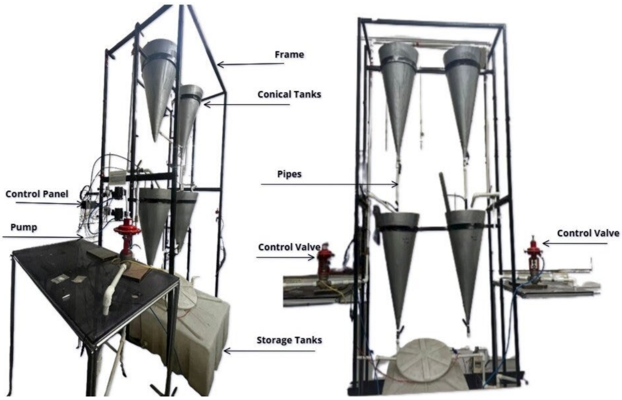

(a)

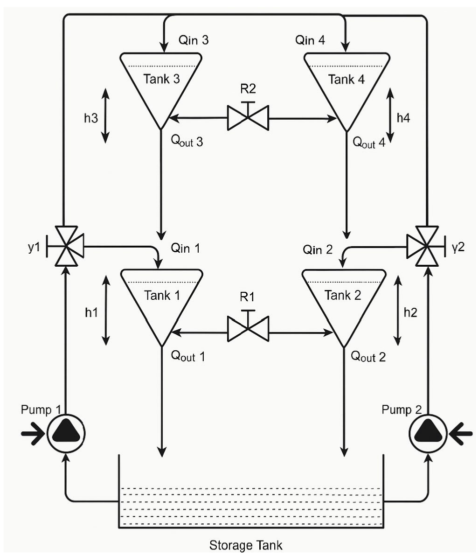

(b)

Fig. 1 – (a) *Quadruple Conical Tank System Setup;*
(b) *Schematic of Quadruple Conical Tank System with interaction.*

The Pump 1 drives the liquid to the Tank 1 and Tank 4 and Pump 2 drives the liquid to the Tank 2 and Tank 3 through a three-way valve. The flow rate of the liquid in the tanks is controlled by the position of the three-way valve which is represented by γ. Thus, by controlling the value of γ, each pump drives the liquid to two tanks, one of the bottom tanks and its diagonally placed tank. The interacting valves R_1 and R_2 creates interaction between Tank 1, Tank 2, Tank 3 and Tank 4 respectively. The degree of interaction varied by changing the values of R_1 and R_2.

If the R_1 and R_2 values are kept "0" then the QCTS is without interaction and when the values of R_1 and R_2 are "1" then the QCTS is with interaction as shown in Fig. 1b. Each tank has a discharge valve at the bottom of all the four tanks. The interface of tanks occurs as the discharge of the Tank 4 pours into Tank 2 and the discharge of the Tank 3 pours into Tank 1. The discharge of Tank 1 and Tank 2 is collected at the reservoir. This interface makes this system a multivariable control system due to its effective coupling. The multivariable control system with increased non-linearity due to conical shape and interaction challenges to identify and control the QCTS. The mathematical modelling of each tank is developed by considering the mass balance equation and Bernoulli's equation gives and solved at different operating points to get the transfer function model.

The parameters of the Conical Quadruple Tank System:
H [cm] – Total Height of conical tank (75 cm),
R – Radius of top of Tank (19 cm),
h – Height of liquid in Tank,
r – Radius of water in Tank,
h_1, h_2, h_3, h_4 – Height of liquid in Tank 1, 2, 3, 4 respectively,
v_1, v_2 [V] – Voltage of pumps 1 and 2,
g_1, g_2 – Flow distribution to the lower and upper diagonal tank of Valve 1 and Valve 2,
$A_i\,[\text{cm}^2] = \left(\pi R^2/H^2\right) h_i^2 = (\alpha)_i^2$ – The cross-sectional area of i^{th} Conical tank,
$V\,[\text{cm}^3]$ – Volume of the conical tank,
$a\,[\text{cm}^2]$ – Cross-sectional area of Pipe,
$Q_{in}\,[\text{cm}^3/\text{s}]$ – Input Pump flow,
$Q_{\text{out}}\,[\text{cm}^3/\text{s}]$ – Output flow,
$g = 981\,[\text{cm/s}]$ – Acceleration due to gravity,
K_1, K_2 – Pump Flow Constant $\left(70.67\,[\text{cm}^3/\text{s}]\right)$,
r_1, r_2, r_3, r_4 – Drain valves of Tank 1, 2, 3, 4 respectively,
γ_1, γ_2 – Diverter Valve Constants,

R_1, R_2 – Manual Valve for Interaction,

a_{12} – Area of the pipe between Tank 1 and Tank 2,

a_{34} – Area of the pipe between Tank 3 and Tank 4.

The final equations without interactions of the all tanks:

$$\frac{\mathrm{d}h_1}{\mathrm{d}t} = \frac{1}{\mathrm{d}h_1^2}\left[\gamma_1 K_1 V_1 + a_3 r_3 \sqrt{2gh_3} - a_1 r_1 \sqrt{2gh_1}\right], \tag{1}$$

$$\frac{\mathrm{d}h_2}{\mathrm{d}t} = \frac{1}{\mathrm{d}h_2^2}\left[\gamma_2 K_2 V_2 + a_4 r_4 \sqrt{2gh_4} - a_2 r_2 \sqrt{2gh_2}\right], \tag{2}$$

$$\frac{\mathrm{d}h_3}{\mathrm{d}t} = \frac{1}{\mathrm{d}h_3^2}\left[\left(1-\gamma_2\right) K_2 V_2 - a_3 r_3 \sqrt{2gh_3}\right], \tag{3}$$

$$\frac{\mathrm{d}h_4}{\mathrm{d}t} = \frac{1}{\mathrm{d}h_4^2}\left[\left(1-\gamma_1\right) K_1 V_1 - a_4 r_4 \sqrt{2gh_4}\right]. \tag{4}$$

The final equations with the interaction for all the tanks:

$$\frac{\mathrm{d}h_1}{\mathrm{d}t} = \frac{1}{h_1^2}\left[\begin{array}{c}\gamma_1 K_1 V_1 + a_3 r_3 \sqrt{2gh_3} + \mathrm{sign}\left(h_3 - h_4\right) R_2 a_{34} r_3 \sqrt{2g\left|h_3 - h_4\right|} - \\ a_1 r_l \sqrt{2gh_1} - \mathrm{sign}\left(h_{1^-} h_2\right) R_1 a_{12} r_1 \sqrt{2g\left|h_{l^-} h_2\right|}\end{array}\right], \tag{5}$$

$$\frac{\mathrm{d}h_2}{\mathrm{d}t} = \frac{1}{h_2^2}\left[\begin{array}{c}\gamma_2 K_2 V_2 + a_4 r_4 \sqrt{2gh_4} + \mathrm{sign}\left(h_3 - h_4\right) R_2 a_{34} r_4 \sqrt{2g\left|h_3 - h_4\right|} \\ -a_2 r_2 \sqrt{2g} h_2 + \mathrm{sign}\left(h_1 - h_2\right) R_1 a_{12} r_2 \sqrt{2g\left|h_1 - h_2\right|}\end{array}\right], \tag{6}$$

$$\frac{\mathrm{d}h_3}{\mathrm{d}t} = \frac{1}{h_3^2}\left[\left(1-\gamma_2\right) K_2 V_{2^-} a_3 r_3 \sqrt{2gh_3} - \mathrm{sign}\left(h_{3^-} h_4\right) R_2 a_{34} r_3 \sqrt{2g\left|h_3 - h_4\right|}\right], \tag{7}$$

$$\frac{\mathrm{d}h_4}{\mathrm{d}t} = \frac{1}{h_4^2}\left[\left(1-\gamma_1\right) K_1 V_{1^-} a_4 r_4 \sqrt{2gh_4} - \mathrm{sign}\left(h_{3^-} h_4\right) R_2 a_{34} r_4 \sqrt{2g\left|h_3 - h_4\right|}\right]. \tag{8}$$

In the case of the interaction the dynamic behavior of QCTS is nonlinear. The linearized state space model using the LabVIEW platform is calculated and considered for the implementation of MPC. The focus of control in this study is on the bottom two tanks (Tank 1 and Tank 2), while the top two tanks serve as intermediate storage feeding into the lower ones with/without coupling effects.

3 Control Scheme for Quadruple Conical Tank System

This paper discusses the implementation of three control scheme for nonlinear process control like PID, Fuzzy and MPC.

3.1 PID Control

The PID control strategy for the QCTS involves calculating the control inputs $u_i(t)$ for each tank based on the error between the desired and actual tank levels. The control input $u_i(t)$ is the manipulated variable, typically the inlet flow rate $q_{in,i}(t)$. Therefore, the PID control law for each tank is:

$$q_{in,i}(t) = K_{p,i} e_i(t) + K_{i,i} \int_0^t e_i(\tau)\, d\tau + K_{d,i} \frac{d e_i(t)}{dt}, \tag{9}$$

where:

$e_i(t) = h_{set,i}(t) - h_i(t)$ is the error for tank i,

$K_{p,i}, K_{i,i}, K_{d,i}$ are the PID gains for tank i,

K_p is the proportional gain,

K_i is the integral gain,

K_d is the derivative gain,

$e(t) = y_{set}(t) - y(t)$ is the error term.

Given the nonlinear nature of the QCTS, it is crucial to consider the varying dynamics of the conical tanks. The nonlinearities arise from the dependence of the cross-sectional area $A_i(h_i)$ and the outlet flow rate $q_{out,i}(t)$ on the tank height $h_i(t)$.

3.2 Fuzzy Logic Control

Fuzzy Logic Control (FLC) is a robust and versatile control strategy that mimics human decision-making processes for handling complex, nonlinear systems. Unlike traditional control methods, FLC does not require a precise mathematical model of the system. Instead, it uses a set of heuristic rules, known as fuzzy rules, to infer the control actions. These rules are based on expert knowledge and are formulated in terms of linguistic variables, which are then translated into actionable outputs through the processes of fuzzification, rule evaluation, and defuzzification [9]. FLC is particularly advantageous for MIMO systems, which are characterized by multiple interacting inputs and outputs. The complexity and nonlinearity of MIMO systems often make conventional control techniques inadequate. FLC addresses these challenges by providing a flexible framework that can accommodate varying system dynamics and interactions.

The first step in designing the FLC is fuzzification, which converts crisp input values into fuzzy values using membership functions. For the QCTS, the primary input variables are the error (e) and the change in error (Δe) of the tank levels.

Following fuzzification, the rule base is developed, consisting of a set of if-then rules derived from expert knowledge and system behavior. These rules map the fuzzy input variables to the desired control actions. Rules are formulated to cover various operating conditions and interactions within the QCTS, ensuring comprehensive and flexible control. The core component that applies the fuzzy rules to the fuzzified inputs to generate fuzzy outputs. This process involves matching the fuzzified inputs to the conditions in the fuzzy rules and combining the results to form the fuzzy output set.

The final step in the FLC design is defuzzification, which converts the fuzzy outputs into control actions. The centroid method, a common defuzzification technique, calculates the centre of gravity of the aggregated fuzzy output set to determine the precise control action. Mathematically, the control action u is given by:

$$u = \frac{\sum_{i=1}^{n} \mu_i u_i}{\sum_{i=1}^{n} \mu_i}, \tag{10}$$

where μ_i represents the membership value of the i-th fuzzy output, and u_i is the corresponding control action.

The fuzzy inference system employs distinct membership functions for the input variables “error” and “change in error,” as well as the output variable “voltage.” Each fuzzy set is defined by its name, shape, and corresponding data points that describe its support and peak characteristics. The membership function for input and output mentioned in graphical structure in Fig. 2.

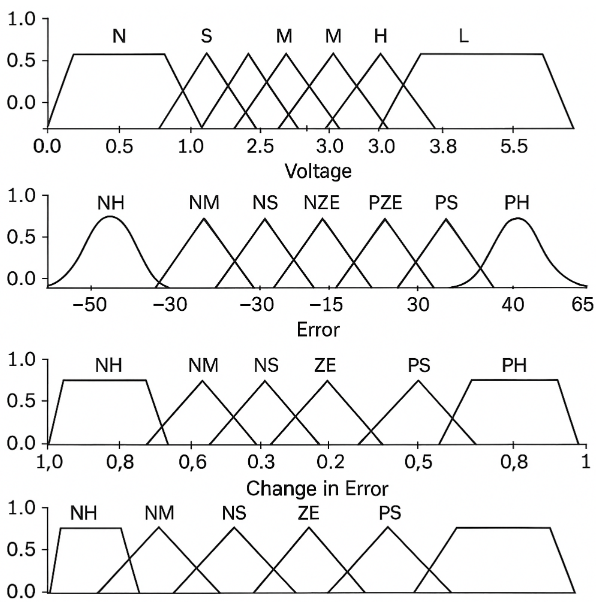

Fig. 2 – *Membership Function for FLC.*

This structured set of membership functions ensures complete coverage and smooth transitions across the range of input and output variables, facilitating accurate and interpretable fuzzy control operations. For an example if error is 60 and change in error is –1 so that large difference between actual and desired level in the tank at that time maximum flow of the pump required. Hence peak voltage needs to be generated to reduce the settling time. A total of 56 fuzzy IF–THEN rules were formulated to define the relationship between the input variables–error and change in error–and the control output voltage. Each rule specifies the control action corresponding to a particular operating condition. **Table 1** shows the some of the examples. For example, IF the error is Negative High (NH) and the change in error is Negative Medium (NM), THEN the output is Negative (N), whereas IF the error is Positive Zero Equivalent (PZE) and the change in error is Negative Medium (NM), THEN the output is Medium (M).

Table 1
Example of Fuzzy rule base.

Rule No.	Error (e)	Rate of Change of Error ($\dot{e}$)	Output (u)	Interpretation / Description
1.	Negative High (NH)	Negative High (NH)	N	Strong negative control action to quickly reduce large negative deviation.
2.	Negative High (NH)	Zero (ZE)	N	Aggressive corrective action to raise process variable toward the set-point.
3.	Zero (ZE)	Zero (ZE)	ZE	No significant control action; system near steady-state.
4.	Positive Small (PS)	Positive Small (PS)	S	Mild positive actuation to avoid overshoot when output is slightly above set-point.
5.	Positive High (PH)	Positive High (PH)	H	Strong positive actuation to counter large positive deviation and fast rising trend.

3.3 Model Predictive Control

MPC is a sophisticated control strategy that offers several advantages, making it particularly suitable for complex systems like the QCTS. One of the key features of MPC is its ability to predict future outputs of the system over a specified prediction horizon. By forecasting the system’s behavior, MPC can make proactive adjustments to maintain optimal performance. This forward-looking approach is essential for managing the dynamic nature of nonlinear systems. Additionally, MPC optimizes a cost function that generally includes terms for both tracking error, which measures how well the system follows the desired setpoints, and control effort, which assesses the energy or resources used to achieve this control. This optimization ensures that the system operates efficiently while maintaining accuracy. Another significant benefit of MPC is its capacity to handle constraints explicitly. This means that MPC can respect the physical and operational limits of the system, such as maximum flow rates or safety boundaries, which are critical for preventing damage or unsafe operation. Furthermore, MPC excels in multi-variable control scenarios, as it is inherently designed to manage multi-input, multi-output (MIMO) systems. This capability allows MPC to handle interactions between multiple control loops effectively, ensuring that the entire system operates cohesively. These characteristics make MPC especially effective for managing the complexities and nonlinearities of systems like the QCTS, where traditional control methods may not provide the necessary precision and adaptability [10].

The prediction model is central to MPC and can be derived from the system's physical principles and identified from experimental data. The model typically takes the form of state-space equations

$$\boldsymbol{x}(k+1) = \boldsymbol{A}\boldsymbol{x}(k) + \boldsymbol{B}\boldsymbol{u}(k), \tag{11}$$

$$\boldsymbol{y}(k) = \boldsymbol{C}\boldsymbol{x}(k), \tag{12}$$

where:

$\boldsymbol{x}(k)$ is the state vector at time step *k*,

$\boldsymbol{u}(k)$ is the control input vector,

$\boldsymbol{y}(k)$ is the output vector,

$\boldsymbol{A}$, $\boldsymbol{B}$ and $\boldsymbol{C}$ are the system matrices.

For nonlinear systems, the model can be nonlinear

$$\boldsymbol{x}(k+1) = f\left(\boldsymbol{x}(k), \boldsymbol{u}(k)\right), \tag{13}$$

$$y(k) = g\left(\boldsymbol{x}(k)\right). \tag{14}$$

Below is a detailed derivation for Model Predictive Control (MPC) modeling. So, from (13), by incrementing step *k*

$$\boldsymbol{x}_{k+2} = \boldsymbol{A}\boldsymbol{x}_{k+1} + \boldsymbol{B}\boldsymbol{u}_{k+1}. \tag{15}$$

Inserting (11) in (13), one can get

$$\boldsymbol{x}_{k+2} = \boldsymbol{A}\left[\boldsymbol{A}\boldsymbol{x}_k + \boldsymbol{B}\boldsymbol{u}_k\right] + \boldsymbol{B}\boldsymbol{u}_{k+1}, \tag{16}$$

$$\boldsymbol{x}_{k+2} = \boldsymbol{A}^2\boldsymbol{x}_k + \boldsymbol{A}\boldsymbol{B}\boldsymbol{u}_k + \boldsymbol{B}\boldsymbol{u}_{k+1}. \tag{17}$$

Consider the linear dynamics as shown in (15)

$$\boldsymbol{x}_{k+1} = \boldsymbol{A}\boldsymbol{x}_k + \boldsymbol{B}\boldsymbol{u}_k, \tag{18}$$

$$\boldsymbol{y}_k = \boldsymbol{C}\boldsymbol{x}_k. \tag{19}$$

For $k=k+1$, the output is

$$\boldsymbol{y}_{k+1}=\boldsymbol{C}\boldsymbol{x}_{k+1}. \tag{20}$$

Substituting the value of $\boldsymbol{x}_{k+1}$ in (20), the equation can be written as

$$\boldsymbol{y}_{k+1}=\boldsymbol{C}\left(\boldsymbol{A}\boldsymbol{x}_k+\boldsymbol{B}\boldsymbol{u}_k\right), \tag{21}$$

$$\boldsymbol{y}_{k+1}=\boldsymbol{C}\boldsymbol{A}\boldsymbol{x}_k+\boldsymbol{C}\boldsymbol{B}\boldsymbol{u}_k. \tag{22}$$

Similarly, for $k=k+2$, the output $\boldsymbol{y}_{k+2}=\boldsymbol{C}\boldsymbol{x}_{k+2}$

$$\boldsymbol{y}_{k+2}=\boldsymbol{C}\left(\boldsymbol{A}\boldsymbol{x}_{k+1}+\boldsymbol{B}\boldsymbol{u}_{k+1}\right), \tag{23}$$

$$\boldsymbol{y}_{k+2}=\boldsymbol{C}\boldsymbol{A}\boldsymbol{x}_{k+1}+\boldsymbol{C}\boldsymbol{B}\boldsymbol{u}_{k+1}, \tag{24}$$

$$\boldsymbol{y}_{k+2}=\boldsymbol{C}\boldsymbol{A}\left[\boldsymbol{A}\boldsymbol{x}_k+\boldsymbol{B}\boldsymbol{u}_k\right]+\boldsymbol{C}\boldsymbol{B}\boldsymbol{u}_{k+1}, \tag{25}$$

$$\boldsymbol{y}_{k+2}=\boldsymbol{C}\boldsymbol{A}^2x_k+\boldsymbol{C}\boldsymbol{A}\boldsymbol{B}\boldsymbol{u}_k+\boldsymbol{C}\boldsymbol{B}\boldsymbol{u}_{k+1}, \tag{26}$$

for $k=k+3$, the output $\boldsymbol{y}_{k+3}=\boldsymbol{C}\boldsymbol{x}_{k+3}$, therefore

$$\boldsymbol{y}_{k+3}=\boldsymbol{C}\left(\boldsymbol{A}\boldsymbol{x}_{k+2}+\boldsymbol{B}\boldsymbol{u}_{k+2}\right), \tag{27}$$

$$\boldsymbol{y}_{k+3}=\boldsymbol{C}\boldsymbol{A}\boldsymbol{x}_{k+2}+\boldsymbol{C}\boldsymbol{B}\boldsymbol{u}_{k+2}, \tag{28}$$

$$\boldsymbol{y}_{k+3}=\boldsymbol{C}\boldsymbol{A}\left[\boldsymbol{A}^2\boldsymbol{x}_k+\boldsymbol{A}\boldsymbol{B}\boldsymbol{u}_k+\boldsymbol{B}\boldsymbol{u}_{k+1}\right]+\boldsymbol{C}\boldsymbol{B}\boldsymbol{u}_{k+2}, \tag{29}$$

$$\boldsymbol{y}_{k+3}=\boldsymbol{C}\boldsymbol{A}^3\boldsymbol{x}_k+\boldsymbol{C}\boldsymbol{A}^2\boldsymbol{B}\boldsymbol{u}_k+\boldsymbol{C}\boldsymbol{A}\boldsymbol{B}\boldsymbol{u}_{k+1}+\boldsymbol{C}\boldsymbol{B}\boldsymbol{u}_{k+2}. \tag{30}$$

Arranging the output equations $\boldsymbol{y}_k, \boldsymbol{y}_{k+1}, \boldsymbol{y}_{k+2}$, and $\boldsymbol{y}_{k+3}$ in terms of matrix

$$\begin{bmatrix}\boldsymbol{y}_k\\ \boldsymbol{y}_{k+1}\\ \boldsymbol{y}_{k+2}\\ \boldsymbol{y}_{k+3}\end{bmatrix}=\begin{bmatrix}\boldsymbol{C}\\ \boldsymbol{C}\boldsymbol{A}\\ \boldsymbol{C}\boldsymbol{A}^2\\ \boldsymbol{C}\boldsymbol{A}^3\end{bmatrix}\boldsymbol{x}_k+\begin{bmatrix}0&0&0\\ \boldsymbol{C}\boldsymbol{B}&0&0\\ \boldsymbol{C}\boldsymbol{A}\boldsymbol{B}&\boldsymbol{C}\boldsymbol{B}&0\\ \boldsymbol{C}\boldsymbol{A}^2\boldsymbol{B}&\boldsymbol{C}\boldsymbol{A}\boldsymbol{B}&\boldsymbol{C}\boldsymbol{B}\end{bmatrix}\begin{bmatrix}\boldsymbol{u}_k\\ \boldsymbol{u}_{k+1}\\ \boldsymbol{u}_{k+2}\end{bmatrix}. \tag{31}$$

The above matrix can be written as

$$\boldsymbol{y}_{k|4}=\boldsymbol{O}_4x_k+\boldsymbol{H}_4^d\boldsymbol{u}_{k|3}, \tag{32}$$

where: $\boldsymbol{y}_{k|4}$ is the output variable matrix

$$\boldsymbol{y}_{k|4}=\left[\boldsymbol{y}_k \quad \boldsymbol{y}_{k+1} \quad \boldsymbol{y}_{k+2} \quad \boldsymbol{y}_{k+3}\right]^{\mathrm{T}}, \tag{33}$$

$\boldsymbol{O}_4$ is the extended observability matrix for the pair ($\boldsymbol{C}$, $\boldsymbol{A}$)

$$\boldsymbol{O}_4=\left[\boldsymbol{C} \quad \boldsymbol{C}\boldsymbol{A} \quad \boldsymbol{C}\boldsymbol{A}^2 \quad \boldsymbol{C}\boldsymbol{A}^3\right]^{\mathrm{T}}, \tag{34}$$

$\boldsymbol{H}_4^d$ is the lower triangular Toeplitz matrix for the matrices $\boldsymbol{C}$, $\boldsymbol{A}$, and $\boldsymbol{B}$

$$H_4^d = \begin{bmatrix} 0 & 0 & 0 \\ CB & 0 & 0 \\ CAB & CB & 0 \\ CA^2B & CAB & CB \end{bmatrix}, \tag{35}$$

$u_{k|3}$ is the input variable matrix

$$u_{k|3} = \begin{bmatrix} u_k \\ u_{k+1} \\ u_{k+2} \end{bmatrix}, \tag{36}$$

when prediction horizon is equal to L the (32) can be written as

$$y_{k|L} = O_L x_k + H_L^d u_{k|L-1}, \tag{37}$$

when $k = k+1$, the (37) can be written as

$$y_{k+1|L} = O_L x_{k+1} + H_L^d u_{k+1|L-1}. \tag{38}$$

Considering $y_{k+1} = C\left(Ax_k + Bu_k\right)$, Substituting into (38)

$$y_{k+1|L} = O_L\left[Ax_k + Bu_k\right] + H_L^d u_{k+1|L-1}, \tag{39}$$

$$y_{k+1|L} = O_L Ax_k + O_L Bu_k + H_L^d u_{k+1|L-1}. \tag{40}$$

Arranging (40) in the form of matrix

$$y_{k+1|L} = O_L Ax_k + \begin{bmatrix} O_L B & H_L^d \end{bmatrix} \begin{bmatrix} u_k \\ u_{k+1|L-1} \end{bmatrix}. \tag{41}$$

Therefore, simplify the above equation and written as

$$y_{k+1|L} = P_L + F_L u_{k|L}, \tag{42}$$

where:

$$P_L = O_L Ax_k, \quad F_L = \begin{bmatrix} O_L B & H_L^d \end{bmatrix}, u_{k|L} = \begin{bmatrix} u_k \\ u_{k+1|L-1} \end{bmatrix}.$$

The (42) is known as the prediction equation or prediction model and model predictive control technique obtains its predicted output by utilizing the (36).

Consider the cost function shown in (43)

$$J_k = \left(y_{k+1|L} - \gamma_{k+1|L}\right)^{\mathrm{T}} Q\left(y_{k+1|L} - \gamma_{k+1|L}\right) + u_{k|L}^{\mathrm{T}} R u_{k|L}. \tag{43}$$

Substituting the prediction (42) in the equation of cost function (43)

$$J_k = \left(P_L + F_L u_{k|L} - \gamma_{k+1|L}\right)^{\mathrm{T}} Q\left(P_L + F_L u_{k|L} - \gamma_{k+1|L}\right) + u_{k|L}^{\mathrm{T}} R u_{k|L}, \tag{44}$$

$$\boldsymbol{J}_k = \left(\boldsymbol{P}_L + \boldsymbol{F}_L \boldsymbol{u}_{k|L} - \boldsymbol{\gamma}_{k+1|L}\right)^{\mathrm{T}} \left(\boldsymbol{Q}\boldsymbol{P}_L + \boldsymbol{Q}\boldsymbol{F}_L \boldsymbol{u}_{k+L} - \boldsymbol{\gamma}_{k+1|L}\right) + \boldsymbol{u}_{k|L}^{\mathrm{T}} \boldsymbol{R} \boldsymbol{u}_{k|L}, \tag{45}$$

$$\begin{aligned} \boldsymbol{J}_k = {} & \boldsymbol{P}_L^T \boldsymbol{Q}\boldsymbol{P}_L + \boldsymbol{P}_L^T \boldsymbol{Q}\boldsymbol{F}_L \boldsymbol{u}_{k|L} - \boldsymbol{P}_L^T \boldsymbol{Q}\boldsymbol{\gamma}_{k+1|L} + \boldsymbol{u}_{k|L}^T \boldsymbol{F}_L^T \boldsymbol{Q}\boldsymbol{P}_L + \boldsymbol{u}_{k|L}^T \boldsymbol{F}_L^T \boldsymbol{Q}\boldsymbol{F}_L \boldsymbol{u}_{k|L} - \\ & - \boldsymbol{u}_{k|L}^T \boldsymbol{F}_L^T \boldsymbol{Q}\boldsymbol{\gamma}_{k+1|L} - \boldsymbol{\gamma}_{k+1|L}^T \boldsymbol{Q}\boldsymbol{P}_L - \boldsymbol{\gamma}_{k+1|L}^T \boldsymbol{Q}\boldsymbol{F}_L \boldsymbol{u}_{k|L} + \boldsymbol{\gamma}_{k+1|L}^T \boldsymbol{Q}\boldsymbol{\gamma}_{k+1|L} + \boldsymbol{u}_{k|L}^{\mathrm{T}} \boldsymbol{R}\boldsymbol{u}_{k|L}, \end{aligned} \tag{46}$$

Arranging (46) the cost function can be written as

$$\begin{aligned} \boldsymbol{J}_k = {} & \boldsymbol{u}_{k|L}^T \left(\boldsymbol{F}_L^T \boldsymbol{Q} F_L + \boldsymbol{R}\right) \boldsymbol{u}_{K|L} + 2\boldsymbol{F}_L^T \boldsymbol{Q}\left(\boldsymbol{P}_L - \boldsymbol{\gamma}_{k+1|L}\right) \boldsymbol{u}_{k|L} + \\ & + \left(\boldsymbol{P}_L - \boldsymbol{\gamma}_{k+1|L}\right)^T \boldsymbol{Q}\left(\boldsymbol{P}_L - \gamma_{k+1|L}\right), \end{aligned} \tag{47}$$

or

$$\boldsymbol{J}_k = \boldsymbol{u}_{k|L}^T \boldsymbol{H} \boldsymbol{u}_{k|L} + 2\boldsymbol{f}^T \boldsymbol{u}_{k|L} + \boldsymbol{J}_0, \tag{48}$$

where

$$\boldsymbol{H} = \boldsymbol{F}_L^T \boldsymbol{Q} F_L + \boldsymbol{R}, \tag{49}$$

$$\boldsymbol{f}^T = \boldsymbol{F}_L^T \boldsymbol{Q}\left(\boldsymbol{P}_L - \boldsymbol{\gamma}_{k+1|L}\right), \tag{50}$$

$$\boldsymbol{J}_0 = \left(\boldsymbol{P}_L - \boldsymbol{\gamma}_{k+1|L}\right)^T \boldsymbol{Q}\left(\boldsymbol{P}_L - \boldsymbol{\gamma}_{k+1|L}\right). \tag{51}$$

To minimize the cost function, taking the derivative of (48) with respect to $u_{k|L}$

$$\frac{\partial \boldsymbol{J}_k}{\partial \boldsymbol{u}_{k|L}} = \frac{\partial}{\partial \boldsymbol{u}_{k|L}} \left(\boldsymbol{u}_{k|L}^T \boldsymbol{H} \boldsymbol{u}_{k|L} + 2\boldsymbol{f}^T \boldsymbol{u}_{k|L} + \boldsymbol{J}_0\right) = 0. \tag{52}$$

Therefore

$$2\boldsymbol{H}\boldsymbol{u}_{k|L} + 2\boldsymbol{f}^{\mathrm{T}} = 0, \tag{53}$$

or

$$2\boldsymbol{H}\boldsymbol{u}_{K|L} = -2\boldsymbol{f}^{\mathrm{T}}, \tag{54}$$

$$\boldsymbol{u}_{k|L} = -\boldsymbol{H}^{-1} \boldsymbol{f}^{\mathrm{T}}, \tag{55}$$

$$\boldsymbol{u}_{k|L} = -\left(\boldsymbol{F}_L^T \boldsymbol{Q} F_L + \boldsymbol{R}\right)^{-1} \boldsymbol{F}_L^T \boldsymbol{Q}\left(\boldsymbol{P}_L - \boldsymbol{\gamma}_{k+1|L}\right). \tag{56}$$

The (56) is the optimal control which will be to predict the future elements

$$\boldsymbol{u}_{k|L} = \left(\boldsymbol{P}_L + \boldsymbol{F}_L \boldsymbol{u}_{k|L} - \boldsymbol{\gamma}_{k+1|L}\right)^{\mathrm{T}} \boldsymbol{Q}\left(\boldsymbol{P}_L + \boldsymbol{F}_L \boldsymbol{u}_{k|L} - \boldsymbol{\gamma}_{k+1|L}\right) + \boldsymbol{u}_{k|L}{}^{\mathrm{T}} \boldsymbol{R} \boldsymbol{u}_{k|L}, \tag{57}$$

$$\boldsymbol{u}_{k|L} = \left(\boldsymbol{P}_L + \boldsymbol{F}_L \boldsymbol{u}_{k|L} - \boldsymbol{\gamma}_{k+1|L}\right)^{\mathrm{T}} \left(\boldsymbol{Q}\boldsymbol{P}_L + \boldsymbol{Q}\boldsymbol{F}_L u_{k|L} - \boldsymbol{Q}\boldsymbol{\gamma}_{k+1|L}\right) + \boldsymbol{u}_{k|L}^{\mathrm{T}} \boldsymbol{R}_{u_{k|L}}, \tag{58}$$

$$\boldsymbol{u}_{k|L} = \boldsymbol{P}_L^{\mathrm{T}}\boldsymbol{Q}\boldsymbol{P}_L + \boldsymbol{P}_L^{\mathrm{T}}\boldsymbol{Q}\boldsymbol{F}_L\boldsymbol{u}_{k|L} - \boldsymbol{P}_L^{\mathrm{T}}\boldsymbol{Q}\boldsymbol{\gamma}_{K+1|L} + \boldsymbol{u}_{k|L}^T\boldsymbol{F}_L^T\boldsymbol{Q}\boldsymbol{P}_L + \boldsymbol{u}_{k|L}^T\boldsymbol{F}_L^T\boldsymbol{Q}\boldsymbol{F}_L u_{k|L} -$$
$$- \boldsymbol{u}_{k|L}^T\boldsymbol{F}_L^T\boldsymbol{Q}\boldsymbol{\gamma}_{K+1|L} - \boldsymbol{\gamma}_{K+1|L}^{\mathrm{T}}\boldsymbol{Q}\boldsymbol{P}_L - \boldsymbol{\gamma}_{K+1|L}^{\mathrm{T}}\boldsymbol{Q}\boldsymbol{F}_L\boldsymbol{u}_{k|L} + \boldsymbol{\gamma}_{K+1|L}^{\mathrm{T}}\boldsymbol{Q}\boldsymbol{\gamma}_{K+1|L} + \boldsymbol{u}_{k|L}^T\boldsymbol{R}\boldsymbol{u}_{k|L}, \tag{59}$$

$$\boldsymbol{u}_{k|L} = \boldsymbol{u}_{k|L}^T(\boldsymbol{F}_L^T\boldsymbol{Q}\boldsymbol{F}_L + \boldsymbol{R})\boldsymbol{u}_{k|L}, \tag{60}$$

$$\boldsymbol{u}_{k|L} = \boldsymbol{P}_L^{\mathrm{T}}\boldsymbol{Q}\boldsymbol{P}_L - \boldsymbol{P}_L^{\mathrm{T}}\boldsymbol{Q}\boldsymbol{\gamma}_{k+1|L} - \boldsymbol{\gamma}_{k+1|L}^{\mathrm{T}}\boldsymbol{Q}\boldsymbol{P}_L + \boldsymbol{\gamma}_{k+1|L}^{\mathrm{T}}\boldsymbol{Q}\boldsymbol{\gamma}_{k+1|L}, \tag{61}$$

$$\boldsymbol{u}_{k|L} = \left(\boldsymbol{P}_L - \boldsymbol{\gamma}_{k+1|L}\right)^T \boldsymbol{Q}\left(\boldsymbol{P}_L - \boldsymbol{\gamma}_{k+1|L}\right), \tag{62}$$

$$\boldsymbol{u}_{k|L} = \boldsymbol{P}_L^{\mathrm{T}}\boldsymbol{Q}\boldsymbol{F}_L\boldsymbol{u}_{k|L} + \boldsymbol{u}_{k|L}^T\boldsymbol{F}_L^T\boldsymbol{Q}\boldsymbol{P}_L - \boldsymbol{u}_{k|L}^T\boldsymbol{F}_L^T\boldsymbol{Q}\boldsymbol{\gamma}_{k+1|L} - \boldsymbol{\gamma}_{k+1|L}^{\mathrm{T}}\boldsymbol{Q}\boldsymbol{F}_L\boldsymbol{u}_{k|L}, \tag{63}$$

$$\boldsymbol{f}^{\mathrm{T}} = \boldsymbol{P}_L\boldsymbol{Q}\boldsymbol{F}_L^{\mathrm{T}} + \boldsymbol{P}_L^{\mathrm{T}}\boldsymbol{Q}\boldsymbol{F}_L - \boldsymbol{F}_L, \tag{64}$$

$$\boldsymbol{J}_0 = 2\boldsymbol{F}_L^{\mathrm{T}}\boldsymbol{Q}\boldsymbol{P}_L - 2\boldsymbol{F}_L^{\mathrm{T}}\boldsymbol{Q}\gamma_{k+1|L}. \tag{65}$$

Therefore, the cost function is

$$\boldsymbol{J}_k = \boldsymbol{u}_{k|L}^{\mathrm{T}} + \boldsymbol{u}_{k|L}2\boldsymbol{f}^{\mathrm{T}}\boldsymbol{u}_{k|L} - \boldsymbol{J}_0. \tag{66}$$

Differentiating above equation with respect to $\boldsymbol{u}_{k|L}$

$$\frac{\partial \boldsymbol{J}_K}{\boldsymbol{u}_{k|L}} = -\boldsymbol{H}^{-1}\boldsymbol{f}^{\mathrm{T}}, \tag{67}$$

$$0 = 2\boldsymbol{H}\boldsymbol{U}_{k|L} + 2\boldsymbol{f}^{\mathrm{T}}, \tag{68}$$

$$-2\boldsymbol{f}^{\mathrm{T}} = 2\boldsymbol{H}\boldsymbol{U}_{k|L}. \tag{69}$$

A linearized model at a single operating point often fails to handle the entire range in Model Predictive Control due to Nonlinearity of the system. Linearizing a QCTS model around a single operating point simplifies the system to a linear approximation, which is only accurate near that point. As the system state moves away from this point, the linear model becomes increasingly inaccurate. Linearization approximates the system's behavior using a Taylor series expansion around an operating point. This approximation is valid only within a small neighborhood of that point. In QCTS, operating conditions vary significantly over time. A linear model derived at a specific operating point does not adapt to these changes, leading to poor performance in predicting and controlling the system under different conditions. MPC with adaptive model switching algorithm is implemented to handle the limitation of linearized modelling.

4 Results and Analysis of Controller Performance on Hardware

In this study, advanced control algorithms were designed and implemented for a nonlinear coupled MIMO system. The primary objective was to evaluate the performance of various controllers, including PID, Fuzzy Logic, and MPC, in managing the system dynamics.

The research is involved in hardware implementation phases. PID controller, Fuzzy Logic controller, and Model Predictive Controller were implemented and tested under different conditions.

The performance of the controllers was assessed through case studies, each corresponding to different set-points.

4.1 Case 1: set-point at 40 cm

In this experiment, the set-point is maintained at 40 cm for both tanks. The level tracking of both tanks and the controller efforts for the three controllers (PID, FLC, and MPC) are analyzed and compared, Figs. 3 and 4.

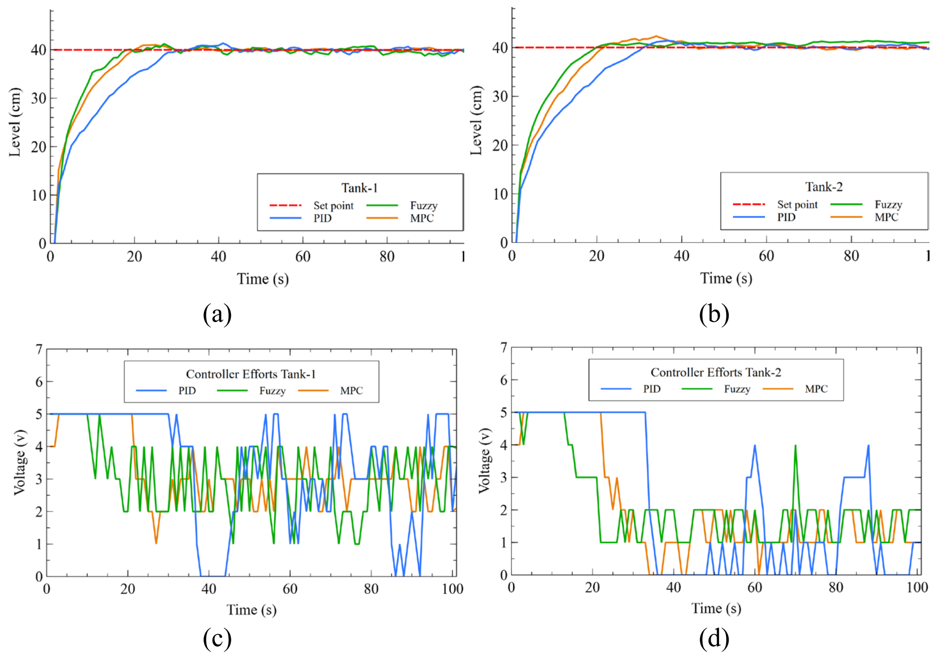

Fig. 3 – *Hardware comparative data for experiments of PID, Fuzzy and MPC at set-point* 40 cm.

As seen in Fig. 3, MPC is better in tracking the setpoint in both tanks as compared to PID and FLC. Also, the controller efforts in the case of MPC controllers are minimal and show lesser fluctuations compared with FLC.

The performance indices in numerical form are shown for PID, FLC, and MPC with respect to both tanks in **Table 2**. It is observed that the performance indicators of the MPC controller and FLC are similar; however, the performance of the PID controller is poor. The MPC controller reaches the set-point in both tanks, whereas PID and FLC settle at around 39 cm in Tank 1. The minimum and maximum settling times, average control action, and average voltage are similar in the case of FLC and MPC. From the results shown in Fig. 3 and **Table 2**, it can be concluded that the performance of the MPC controller is comparatively better than PID and FLC controllers. Error response shown in Fig. 4.

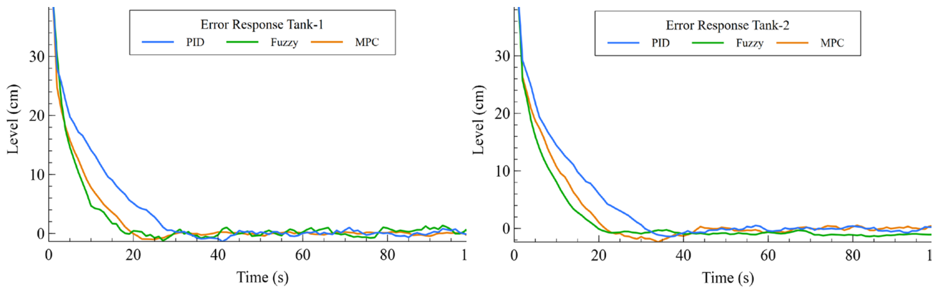

(a) (b)

Fig. 4 – *Error response for both the tanks at set-point* 40 cm.

Table 2

Comparison of PID, Fuzzy, and MPC Controllers for Set point Tracking at 40 cm.

Sr. No.	Performance Index details	PID		Fuzzy		MPC	
		Tank 1	Tank 2	Tank 1	Tank 2	Tank 1	Tank 2
1.	Rise Time (s)	21.71	21.34	10.78	12.07	13.07	12.07
2.	Settling Minimum Value (cm)	36.62	36.10	36.40	36.61	36.43	36.61
3.	Settling Maximum Value (cm)	41.36	41.43	41.22	41.39	41.00	41.39
4.	Overshoot (%)	3.40	3.55	3.07	3.48	2.50	3.48
5.	Undershoot (%)	0					
6.	Peak Value (cm)	41.36	41.42	41.22	41.39	41.00	41.39
7.	Peak Time (s)	41.00	37.00	27.00	84.00	25.00	84.00
8.	Average of Square Error (cm^2)	54.51	68.03	39.81	41.66	39.54	50.30
9.	Average of Voltage (V)	3.35	2.00	3.95	2.06	2.10	2.10
10.	Average of Control Action (V)	2.67		3.00		2.10	

4.2 Case 2: set-point at 50 cm

In this experiment, the set-point is maintained at 50 cm for both tanks. The level tracking of both tanks and the controller efforts for the three controllers (PID, Fuzzy, and MPC) are analyzed and compared. As seen in Fig. 5, MPC is better in tracking the setpoint in both tanks as compared to PID and FLC. Also, the controller efforts in the case of MPC controllers are minimal and show lesser fluctuations compared with FLC. The performance indices in numerical form are shown for PID, FLC, and MPC with respect to both tanks in **Table 3**. It is observed that the performance indicators of the MPC controller and FLC are similar. However, the performance of the PID controller is poor. The MPC controller reaches the set-point in both tanks. The minimum and maximum settling times, average control action, and average voltage are similar in the case of FLC and MPC. From the results shown in Fig. 6 and **Table 3**, it can be concluded that the performance of the FLC controller is comparatively better than PID and MPC.

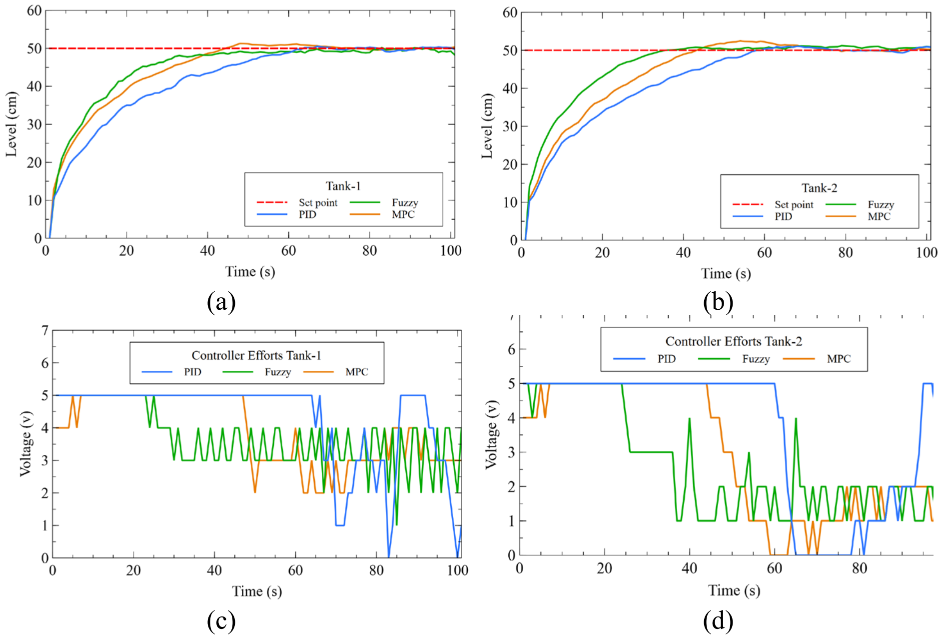

Fig. 5 – *Hardware comparative data for experiments of PID, Fuzzy and MPC at set-point* 50 cm.

Table 3

Comparison of PID, Fuzzy, and MPC Controllers for Set-point Tracking at 50 cm.

Sr. No.	Performance Index details	PID		Fuzzy		MPC	
		Tank 1	Tank 2	Tank 1	Tank 2	Tank 1	Tank 2
1.	Rise Time (s)	44.40	22.36	22.11	21.36	29.67	30.56
2.	Settling Minimum Value (cm)	45.27	44.21	45.22	45.21	45.57	45.58
3.	Settling Maximum Value (s)	51.37	51.82	50.16	51.21	51.29	52.49
4.	Overshoot (%)	2.75	2.53	0.32	2.43	2.58	4.98
5.	Undershoot (%)	0					
6.	Peak Value (cm)	51.37	41.39	50.16	51.21	51.29	52.49
7.	Peak Time (s)	83.00	84.00	83.00	79.00	48.00	54.00
8.	Average of Square Error (cm^2)	169.4	184.78	107.15	97.35	121.55	148.85

9.	Average of Voltage (V)	4.28	3.54	3.68	2.53	3.84	2.87
10.	Average of Control Action (V)	3.91		3.105		3.355	

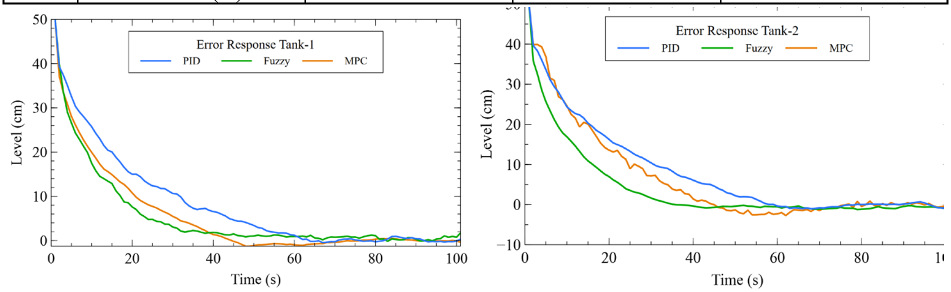

Fig. 6 – *Error response for both the tanks at set-point* 50 cm.

4.3 Case 3: set-point at 60 cm

In this experiment, the set-point is maintained at 60 cm for both tanks. The level tracking of both tanks and the controller efforts for the three controllers (PID, FLC, and MPC) are analyzed and compared.

As seen in Fig. 7, MPC is better in tracking the setpoint in both tanks as compared to PID and FLC. Also, the controller efforts in the case of MPC controllers are minimal and show lesser fluctuations compared with FLC. The performance indices in numerical form are shown for PID, FLC, and MPC with respect to both tanks in **Table 4**.

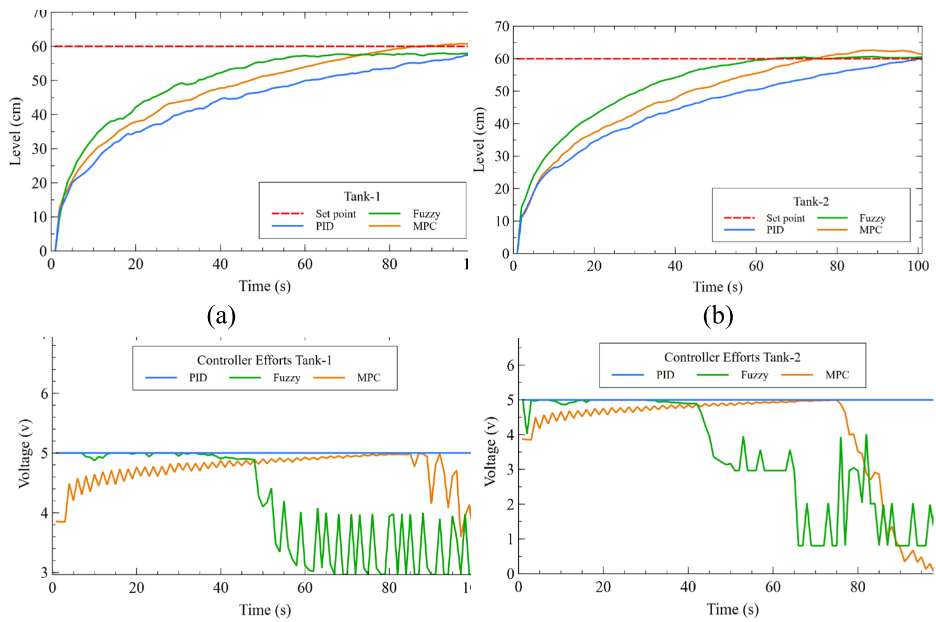

(c) (d)

Fig. 7 – *Hardware comparative data for experiments of PID, Fuzzy and MPC at set-point* 60 cm.

The MPC controller reaches the set-point in both tanks, whereas PID and FLC settle at around 58 cm in Tank 1. The minimum and maximum settling times, average control action, and average voltage are similar in the case of FLC and MPC. From the results shown in Fig. 8 and **Table 4**, it can be concluded that the performance of the MPC controller is comparatively better than PID and FLC.

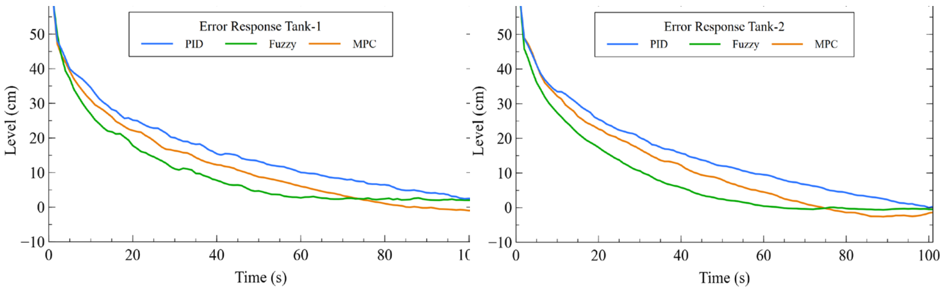

Fig. 8 – *Error response for both the tanks at set-point* 60 cm.

Table 4

Comparison of PID, Fuzzy, and MPC Controllers for Set-point Tracking at 60 cm.

Sr. No.	Performance Index details	PID		Fuzzy		MPC	
		Tank 1	Tank 2	Tank 1	Tank 2	Tank 1	Tank 2
1.	Rise Time (s)	80.15	71.70	44.70	38.06	58.70	53.30
2.	Settling Minimum Value (cm)	54.16	54.18	54.43	54.18	54.19	54.04
3.	Settling Maximum Value (s)	57.85	60.02	57.99	60.62	60.98	62.62
4.	Overshoot (%)	0	0.03	0	1.03	1.60	4.37
5.	Undershoot (%)	0					
6.	Peak Value (cm)	57.85	60.02	57.99	60.62	60.98	62.62
7.	Peak Time (s)	101.00	100.00	100.00	89.00	100.00	89.00
8.	Average of Square Error (cm^2)	383.14	391.34	237.42	222.75	307.16	323.22
9.	Average of Voltage (V)	5.00	4.99	4.17	1.85	4.71	2.85
10.	Average of Control Action (V)	5.00		3.01		3.78	

The results clearly indicate the superiority of the MPC in managing the dynamics of the QCTS nonlinear coupled MIMO system. MPC's ability to anticipate future errors and adjust control actions accordingly enables it to outperform traditional PID and Fuzzy controllers. This is particularly evident in scenarios requiring precise control and minimal overshoot.

The findings from this study provide significant insights into the application of advanced control algorithms in complex systems. The successful implementation and testing of these controllers highlight their potential for broader industrial applications, particularly in processes requiring stringent control specifications.

4.4 Variable set-point profile 1

Fig. 9 shows the performance comparison of three control strategies PID, FLC, and MPC for set-point tracking and control effort in Tank 1. The graph illustrates the level response of Tank 1 over time as it attempts to follow a series of set-point changes. The PID controller shows a relatively fast response but with significant oscillations around the set points. It often overshoots the set point before stabilizing, which suggests aggressive tuning or high gain values. The PID response shown in blue colour tends to have more variability, especially around set-point changes, indicating less stability in its tracking ability. The FLC response shown in green colour provides smoother transitions between set points compared to the PID controller, with fewer oscillations. It follows the set points more consistently, with moderate adjustments that result in reduced overshoot and smoother tracking. This indicates that FLC has a better capacity for handling nonlinearities in the system. The MPC response shown in orange colour is the most stable among the three, with minimal overshoot and smooth transitions to each set point. It maintains close adherence to the set points with fewer oscillations and less variability compared to both PID and FLC. This reflects MPC's ability to predict and optimize control actions over time, resulting in effective set-point tracking.

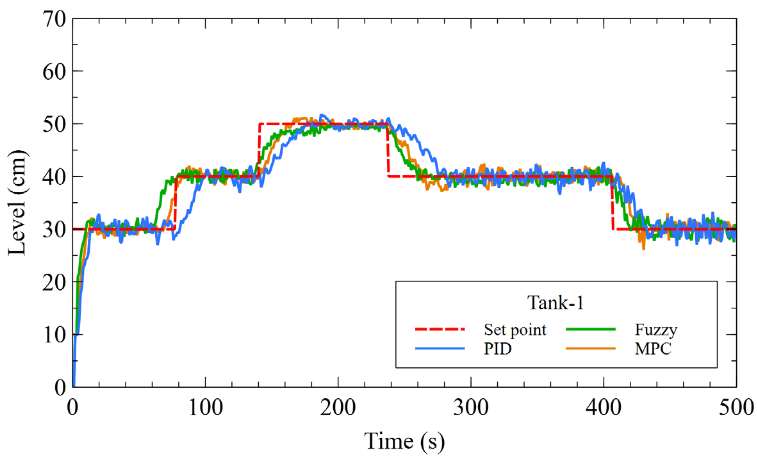

Fig. 9 – *Setpoint tracking response for Tank 1 – MPC, FLC and PID controller.*

The control efforts in terms of voltage applied by each controller over time are shown in Fig. 10. The PID controller exhibits highly variable control effort with frequent and large fluctuations, which reflects its aggressive approach to achieving the set point. This high variability can strain the actuator and reduce system efficiency. The FLC control effort is less variable than PID but still shows moderate fluctuations. The FLC applies control adjustments that are more stable than PID, reflecting its smoother set-point tracking but with periodic adjustments. The MPC control effort is the smoothest of the three, with minimal fluctuations. This suggests that MPC requires fewer and more calculated adjustments to maintain the set point, leading to energy-efficient and stable control action. MPC demonstrates the best set-point tracking performance, followed by FLC, with PID showing the most variability and overshoot. The MPC offers the smoothest and most stable control effort, while PID shows significant fluctuations, and FLC is moderate. The MPC provides more stable and efficient control with fewer adjustments, indicating optimal control performance. FLC also shows good performance with moderate control effort, whereas PID is less efficient due to high variability in its control actions. The comparison shows that MPC outperforms FLC and PID in terms of both set-point tracking and control effort stability, making it the most effective controller for Tank 1 in this setup. The Fuzzy Logic Controller provides a balanced performance with smooth tracking and moderate control effort, while the PID controller, though responsive, exhibits high variability and less stability.

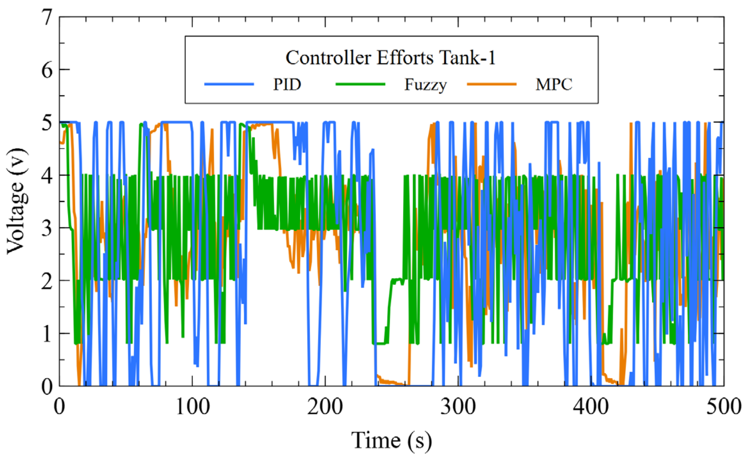

Fig. 10 – *Controller efforts for Tank 1.*

Figs. 11 and 12 illustrates the set-point tracking and control efforts for Tank 2 using three controllers PID, FLC, and MPC over a period of 500 s. The red dashed line indicates changes in the set point at various intervals, representing levels that each controller aims to track. The PID controller response shown in blue colour quickly to set-point changes but displays noticeable overshoot and oscillations around the target levels.

The response, while fast, lacks stability, with significant fluctuations during transitions, suggesting that the PID controller tends to overcompensate and introduces variability around the set point. The FLC response shown in green colour offers smoother tracking with fewer oscillations than PID, closely following set-point changes with minimal overshoot. It maintains a balance between responsiveness and stability, effectively handling nonlinearities in the system and providing consistent tracking across different set points.

MPC response shown in orange colour provides the smoothest and most precise tracking, closely following each set-point change with minimal overshoot and almost no oscillation.

The controller manages transitions smoothly, reflecting its ability to anticipate and optimize control actions. This results in high stability and accurate adherence to set points, making MPC the most effective among the three.

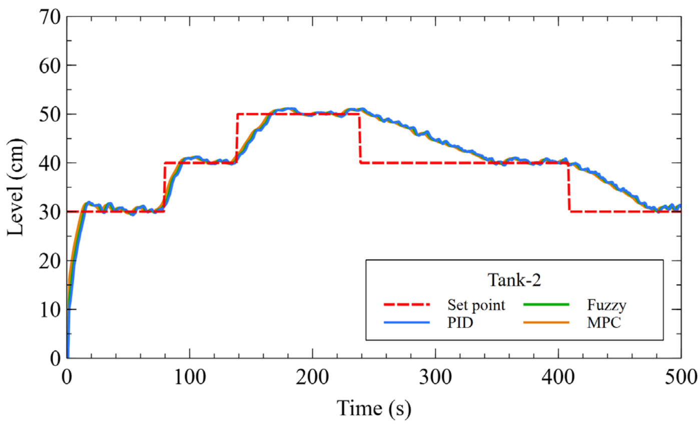

Fig. 11 – *Setpoint tracking response for Tank 2- MPC, FLC and PID controller.*

The PID control effort shows high variability, with frequent and large oscillations in voltage, reflecting its aggressive approach to error correction. This pattern suggests that PID continuously makes large adjustments, which can increase energy consumption and strain on the actuator. FLC exhibits more stable control efforts than PID, with fewer and smaller fluctuations. This indicates that FLC makes calculated adjustments, avoiding the aggressive behavior of PID, thus supporting a more energy-efficient and stable response. MPC has the smoothest control effort with minimal fluctuations, showing its predictive capabilities and efficient adjustments. The steady control effort from MPC suggests optimized energy use and minimal actuator strain due to fewer, more consistent adjustments.

MPC offers the best set-point tracking, followed by FLC, with PID showing the most variability. MPC provides the smoothest and most stable control effort, FLC achieves moderate stability, and PID exhibits the highest variability and aggressiveness. MPC's steady control effort reflects efficient operation, with FLC also performing efficiently but requiring slightly more adjustments. PID is less efficient due to its high variability. For Tank 2, the MPC controller is the most accurate and stable option for set-point tracking, with minimal variability in control effort, making it ideal for applications that require precision and efficiency. The FLC also performs well, providing stable tracking with moderate control effort. Although the PID controller is responsive, it is less stable and energy-efficient due to its aggressive and variable control actions.

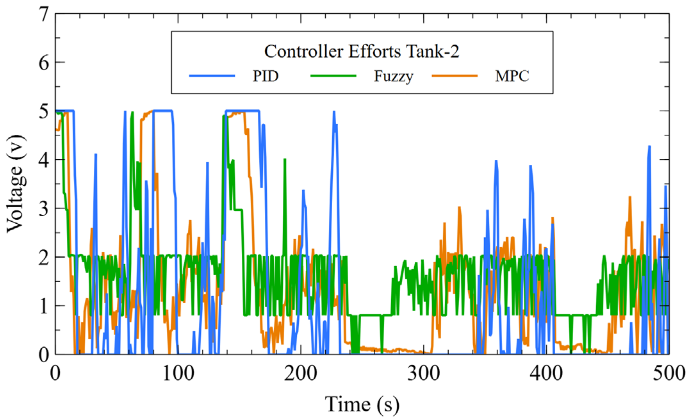

Fig. 12 – *Controller effort for Tank 2.*

5 Conclusion

This research investigated the design, implementation, and comparative performance evaluation of three control algorithms–PID, Fuzzy Logic Control (FLC), and Model Predictive Control (MPC)–on a nonlinear, coupled Multi-Input Multi-Output (MIMO) system: the Quadruple Conical Tank System (QCTS). The primary objective was to assess each controller's effectiveness in real-time hardware scenarios through a series of case studies with fixed and variable set-point profiles.

The hardware implementation demonstrated that the PID controller, while simple and fast in response, exhibited significant oscillations, overshoot, and high control effort variability. These traits highlight the limitations of PID control in managing the nonlinearities and interdependencies inherent in the QCTS. The Fuzzy Logic Controller performed better in terms of smoother transitions and reduced oscillations, particularly evident in fixed set-point cases. FLC's rule-based framework offered improved adaptability to the nonlinear system characteristics. However, the controller still required moderate control effort and exhibited occasional deviations in tracking performance.

Model Predictive Control consistently outperformed both PID and FLC across all test scenarios. It demonstrated superior tracking accuracy, minimal overshoot, and the smoothest control effort profiles for both tanks. The predictive nature of MPC, which considers future system behavior and optimizes control actions accordingly, enabled it to handle set-point variations with greater precision and stability. This was particularly evident in variable set-point profiles, where MPC maintained close adherence with minimal fluctuations, reflecting high efficiency and actuator friendliness. Quantitative performance indices–such as rise time, settling range, average squared error, and average control voltage–corroborated the qualitative observations. MPC showed the best trade-off between response quality and energy efficiency, making it the most suitable control strategy for the QCTS. In conclusion, the findings clearly establish MPC as the most robust and efficient control solution for nonlinear coupled MIMO processes such as the QCTS. The study reinforces the applicability of advanced model-based control techniques in industrial environments where precision, stability, and energy-efficient operation are critical. Future work may focus on hybrid control schemes, adaptive tuning, or real-time embedded deployment to further enhance performance and scalability.

6 Acknowledgments

This work has been supported by Nirma University, Ahmedabad, Gujarat, India.

7 References

[1] J. Xie, F. Bonassi, R. Scattolini: Internal Model Control Design for Systems Learned by Control Affine Neural Nonlinear Autoregressive Exogenous Models, arXiv:2402.05607v2 [eess.SY], January 2025, pp. 1 – 13.

[2] S. Joe Qin, T. A. Badgwell: A Survey of Industrial Model Predictive Control Technology, Control Engineering Practice, Vol. 11, No. 7, July 2003, pp. 733 – 764.

[3] T. Raff, S. Huber, Z. K. Nagy, F. Allgower: Nonlinear Model Predictive Control of a Four Tank System: An Experimental Stability Study, Proceedings of the IEEE International Conference on Control Applications, Munich, Germany, October 2006, pp. 237 – 242.

[4] V. Chaudhari, B. Tamhane, S. Kurode: Robust Liquid Level Control of Quadruple Tank System - Second Order Sliding Mode Approach, IFAC-PapersOnLine, Vol. 53, No. 1, 2020, pp. 7 – 12.

[5] S. Dutta: Optimization in Chemical Engineering, Cambridge University Press, Delhi, 2016.

[6] K. H. Johansson: The Quadruple-Tank Process: A Multivariable Laboratory Process with an Adjustable Zero, IEEE Transactions on Control Systems Technology, Vol. 8, No. 3, May 2000, pp. 456 – 465.

[7] S. K. Lakshmanaprabu, N. Sivaramakrishnan, U. Sabura Banu: Closed Loop Control of Quadruple Tank Process Using Fuzzy Logic PI Controller, International Journal of Computer Applications, pp. 20 – 24.

[8] V. Sánchez-Zurita, G. Pérez-Zuñiga, J. Sotomayor-Moriano: Reconfigurable Model Predictive Control Applied to the Quadruple Tank Process, Proceedings of the 15th European Workshop on Advanced Control and Diagnosis (ACD), Bologna, Italy, November 2019, pp. 937 – 957.

[9] J. J. Vignesh, P. S. Manoharan, J. Vijay Anand: Model Predictive Control of Quadruple Tank System, Proceedings of the IEEE International Conference on Intelligent Techniques in Control, Optimization and Signal Processing (INCOS), Tamilnadu, India, April 2019, pp. 1 – 5.

[10] A. Abdullah, M. Zribi: Control Schemes for a Quadruple Tank Process, International Journal of Computers Communications & Control, Vol. 7, No. 4, November 2012, pp. 594-605.

[11] Z. S. Hashim, H. I. Khani, A. T. Azar, Z. I. Khan, D. A. Smait, A. Abdulwahab, A. M. Zalzala, A. Ja'afar Mohamad Jawad, S. Ahmed, I. Kasim Ibraheem, A. A. Najm, S. M. Fati, M. Tounsi, A. R. Mahlous: Robust Liquid Level Control of Quadruple Tank System: A Nonlinear Model-Free Approach, Actuators, Vol. 12, No. 3, March 2023, p. 119.

[12] Z. Zidane: Constrained Model Predictive Control for the Quadruple-Tank Process, International Advanced Researches and Engineering Journal, Vol. 3, No. 3, December 2019, p. 175 – 181.

[13] N. Muthukumar, V. Gomathi, K. Ramkumar, G. Balasubramanian: Prediction Based Optimal Control of a Quadruple Tank Process, Proceedings of the International Conference on Circuits, Power and Computing Technologies (ICCPCT), Nagercoil, India, March 2013, pp. 685 – 690.

[14] J. Jayaprakash, T. SenthilRajan, T. Harish Babu: Analysis of Modelling Methods of Quadruple Tank System, International Journal of Advanced Research in Electrical, Electronics and Instrumentation Engineering, Vol. 3, No. 8, August 2014, pp. 11552 – 11565.